Proc. Natl. Acad. Sci. USA
Vol. 91, pp. 742–746, January 1994
Medical Sciences

Hyperuricemia and urate nephropathy in urate oxidase-deficient mice

(gene targeting/animal model)

XIANGWEI WU*†, MAKI WAKAMIYA*, SUKESHI VAISHNAV*‡, ROBERT GESKE§, CHARLES MONTGOMERY, JR.§, PAMELA JONES*‡, ALLAN BRADLEY*‡, AND C. THOMAS CASKEY*‡

*Institute for Molecular Genetics, ‡Howard Hughes Medical Institute, and §Center of Comparative Medicine, Baylor College of Medicine, Houston, TX 77030

Contributed by C. Thomas Caskey, October 1, 1993

ABSTRACT **Urate oxidase, or uricase (EC 1.7.3.3), is a purine metabolic enzyme that catalyzes the conversion of uric acid to allantoin in most mammals except humans and certain other primates. The loss of urate oxidase in the human during primate evolution predisposes man to hyperuricemia, a metabolic disturbance that can lead to gouty arthritis and renal stones. To create a mouse model for hyperuricemia and gout, and to address the question of whether urate oxidase is essential in lower mammalian species, we have disrupted the urate oxidase gene in the mouse by homologous recombination in embryonic stem cells. Unlike the human situation, urate oxidase deficiency in mice causes pronounced hyperuricemia and urate nephropathy. More than half of the mutant mice died before 4 weeks of age, indicating that urate oxidase is essential in mice. These mutant mice may also serve as animal models for hyperuricemia and its related nephropathy in humans.**

The end product of purine metabolism varies among species (1–3). Most mammals excrete allantoin because they have an enzyme, urate oxidase (EC 1.7.3.3), which degrades the sparingly soluble uric acid to a more soluble allantoin. Urate oxidase was lost in humans and certain other primates by deleterious mutations in the urate oxidase gene (4). As a result, uric acid is the end product of purine metabolism in these species and uric acid levels approach the saturation point (2, 3). Renal excretion of uric acid is therefore essential.

Elevated uric acid levels are associated with several metabolic disorders such as gouty arthritis and renal stones in humans (5, 6). Unlike most other mammals, humans are predisposed to the development of these diseases through lack of urate oxidase. The degradation of uric acid by urate oxidase leads to very low levels of uric acid in most other mammals and makes them unsuitable as experimental models for human hyperuricemia. The generation of urate oxidase-deficient mice by homologous recombination in mouse embryonic stem (ES) cells may provide a good animal model system to study this common disease and to develop more effective treatments.

Although it is clear that urate oxidase was lost in humans and a few other species by genetic mutations during the evolution of primates (4), the biological function and the evolutionary significance of this loss remain unclear. It has been debated whether this loss provided evolutionary advantages or was simply an evolutionary accident (7–10). To determine whether urate oxidase is an essential enzyme in lower mammals and to develop a model for human hyperuricemia, we generated mice with a targeted mutation at the urate oxidase locus by gene targeting in ES cells. This mutation resulted in a complete loss of urate oxidase activity and a 10-fold increase in the serum uric acid level. These mutant mice developed pronounced hyperuricemia and obstructive nephropathy resulting from uric acid crystals. The accumulation of uric acid also led to early death in 65% of the mutant mice, which may be preventable with the administration of allopurinol, a xanthine oxidase inhibitor.

MATERIALS AND METHODS

Plasmid Construction and ES Cell Culture. Genomic clones of the mouse urate oxidase gene were isolated from a C57BL/6J mouse genomic library by using a mouse cDNA probe, and the gene structure was characterized (X.W., unpublished results). A gene replacement-type vector, pUTK, was constructed as follows. A 6.6-kb *Bgl* II fragment containing exons 2–4 of the mouse gene was cloned into the *Bam*HI site of the pBluescript SK vector (Stratagene). A pMC1neo cassette (11), containing a neomycin-resistance gene (*neo*), was inserted into the *Xho* I site in exon 3, and a herpes simplex virus (HSV) thymidine kinase gene (*tk*) was cloned into a *Sal* I site at one end of the urate oxidase sequence (12). AB1 ES cells (13) were used, and the procedures for culturing ES cells were adopted from Robertson (14).

DNA Electroporation and Identification of Targeted Clones. pUTK DNA was digested with the restriction enzyme *Xho* I to release the plasmid sequence prior to electroporation. The DNA was introduced into ES cells by electroporation (13, 15) and the cells were seeded in 24-well plates. The neomycin analogue G418 (effective concentration, 150 μg/ml) and 1-(2-deoxy-2-fluoro-β-D-arabinofuranosyl)-5-iodouracil (0.2 μM) were added 24 hr later; cells were maintained in selection medium for 10–11 days. Colonies from each well (between 10 and 20) were pooled by treatment with trypsin. An aliquot (about 1/10th) of the cells was used for polymerase chain reaction (PCR) analysis and the remaining cells were stored in Dulbecco's modified Eagle's medium with 10% fetal bovine serum and 10% dimethyl sulfoxide (freezing medium) at −80°C. Individual positive clones were purified from PCR-positive pools by serial dilution, and successful gene-targeting events were confirmed by Southern analysis.

Assay for Urate Oxidase Activity and Uric Acid. A crude extract enriched for urate oxidase was prepared from liver (16). Urate oxidase activity was determined spectrometrically by measuring the rate of consumption of uric acid (17). Uric acid and allantoin levels were measured as described (18, 19).

Histology. Tissues were fixed with either neutral buffered 10% formalin (Surgipath Medical, Richmond, IL), absolute ethanol, or Zenker's solution. After fixation, the tissues were trimmed, dehydrated, and infiltrated with paraffin wax. Sections of the tissue were stained with hematoxylin and eosin. Additional sections were taken of ethanol-fixed tissues. After

The publication costs of this article were defrayed in part by page charge payment. This article must therefore be hereby marked "*advertisement*" in accordance with 18 U.S.C. §1734 solely to indicate this fact.

Abbreviations: ES cell, embryonic stem cell; *neo*, neomycin-resistance gene; *tk*, thymidine kinase gene.

†Present address: Department of Molecular Biology, Princeton University, Princeton, NJ 08544.

paraffin removal these sections were placed in absolute ethanol and stained with an ethanolic eosin solution. Uric acid deposits were either stained with Gomori's silver method or viewed under polarized light to assess anisotropism (20).

Administration of Allopurinol. Allopurinol (Sigma) at various concentrations was administrated continuously in the drinking water to homozygous targeted mutants, including homozygous breeding pairs.

RESULTS

Targeted Disruption of Urate Oxidase Gene in Mice. A replacement vector with the neomycin selection cassette inserted into exon 3 of the urate oxidase gene was constructed (Fig. 1). This insertion disrupted the open reading frame at amino acid 107. The vector DNA was introduced into the AB1 ES cells by electroporation (13), yielding a 2- to 5-fold enrichment for neo^+tk^- recombinants after selection with G418 and 1-(2-deoxy-2-fluoro-β-D-arabinofuranosyl)-5-iodouracil. The resulting ES cells were screened as pools by PCR for a homologous recombination-specific junction fragment. PCR-positive clones were purified from the pools and individual clones were analyzed by Southern blotting (Fig. 2*A*). The frequency of gene targeting at the urate oxidase locus was ≈1/1500 of total neo^+ recombinants.

Several targeted ES clones were injected into C57BL/6J mouse blastocysts to create chimeras. Five male chimeras were generated from clone U27-5, with donor cell contribution from 50% to over 90%, as estimated by coat color.

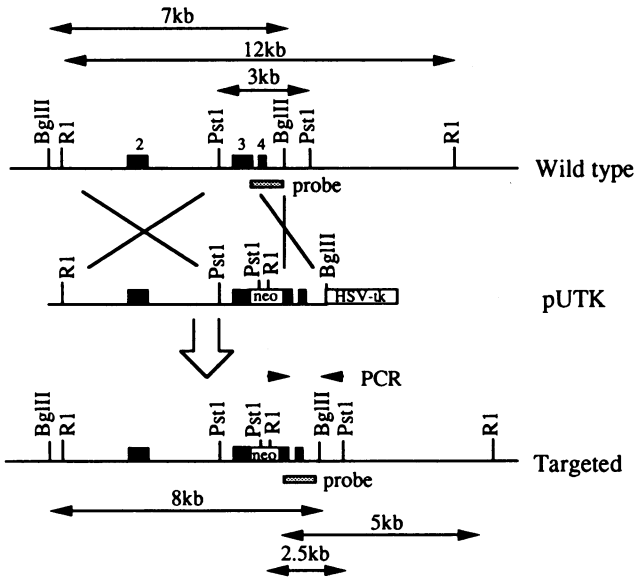

Expected Patterns (kb)

	EcoR1	BglII	Pst1
Wild type	12	7	3
Targeted	5	8	2.5

FIG. 1. Urate oxidase homologous recombination pathway and expected restriction digestion patterns. Restriction maps of the gene-targeting vector pUTK, the wild-type urate oxidase gene locus, and the targeted allele are shown. Exons are indicated by filled, numbered boxes. The *neo* insertion separated the urate oxidase gene into 1.5-kb and 5.1-kb fragments. Primers for PCR amplification of the short arm of homologous recombination junction are indicated by arrows. The probe used in the Southern analysis (shown as the hatched box) lies within the short-arm fragment. R1, *Eco*RI; HSV, herpes simplex virus.

Germ-line transmission was achieved in all five chimeras, with 100% transmission in three cases. Southern analysis of DNA from offspring of heterozygous matings identified mice homozygous for the targeted allele (Fig. 2*B*).

Urate Oxidase Gene Targeting Causes Lethality in Mice. Heterozygous animals displayed no phenotypic abnormality. The heterozygous mice were intercrossed to generate homozygous targeted mutants. Fewer than expected numbers of homozygous mutants were identified at 3 weeks of age (8 out of 112). The few surviving male and female animals were viable and fertile. Matings between homozygous animals with a hybrid genetic background of C57BL/6J and 129Sv produced normal litter sizes (6 to 9 pups) at birth, but of 150 offspring that were born, 97 (65%) died within 4 weeks of age. No losses were observed in control wild-type matings. There is a possibility that variation in rates of lethality is due to the genetic background of the mice. The highest rate of lethality was found on the 129Sv inbred background. On this genetic background only 3 homozygous mutants were found out of 99 offspring generated from heterozygous matings at 3–4 weeks. Further studies using the 129Sv background will be needed to clarify this possibility.

The Insertion in the Urate Oxidase Gene Is a Null Mutation. To test whether the *neo* insertion into the urate oxidase gene created a null mutation, urate oxidase activity was measured in liver extracts. There was significant activity in both wild-type and heterozygous mice, but no detectable activity

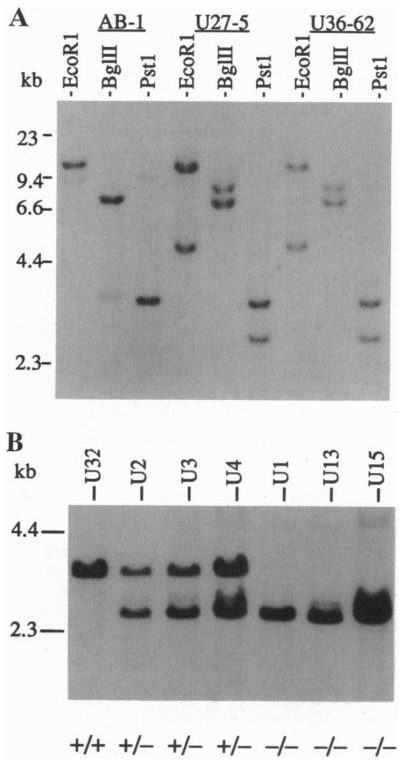

FIG. 2. Southern analysis of ES cell clones for detection of urate oxidase gene targeting and germ-line transmission. (*A*) Identification of targeted ES cell clones. DNA isolated from both wild-type ES cells (AB1) and two PCR-positive clones (U27-5 and U36-62) was digested with *Bgl* II, *Pst* I, or *Eco*RI. The two PCR-positive clones showed the predicted restriction digestion patterns for gene targeting. The faint bands seen in the AB1 DNA are probably due to nonspecific hybridization, since they are not present in other DNA samples. (*B*) Identification of homozygous targeted mice. DNA from the tails of mice generated from heterozygous matings was digested with *Pst* I and probed with the short-arm probe. The 3.0-kb (upper) band represents the wild-type allele and the 2.5-kb (lower) band is the targeted allele. The normal urate oxidase gene allele (wild type) is indicated by +, and − indicates the targeted allele (mutant).

in homozygous mutants (Fig. 3*A*). Urate oxidase protein was also purified from liver extracts. Consistent with the fact that there was no enzyme activity in mutant mice, urate oxidase protein was not detectable (Fig. 3*B*). Compared with their wild-type littermates, heterozygous mice showed a lower specific enzyme activity and a decreased protein level, suggesting a dosage effect of the urate oxidase gene.

A Significant Increase in Uric Acid Is Caused by the Inactivation of Urate Oxidase. As there is no urate oxidase in the homozygous mutants, uric acid was expected to accumulate. This was confirmed by measurement of serum and urinary uric acid (Fig. 4). The serum uric acid of the homozygous mutants reached 11.0 ± 1.7 mg per 100 ml, 10-fold higher than that of wild-type and heterozygous mice and about twice the value found in normal humans (22). No significant difference in uric acid levels was found between heterozygous (1.4 ± 0.5) and wild-type mice (0.9 ± 0.3). In addition to the increase in uric acid in the mutant mice, a decrease in allantoin was observed, indicating that the specific metabolic pathway between uric acid and allantoin was blocked.

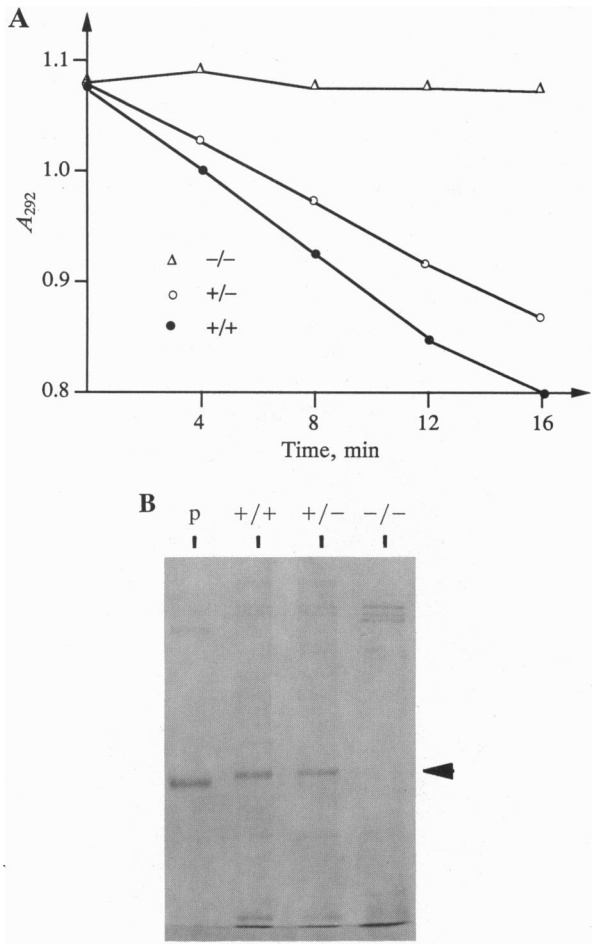

FIG. 3. Undetectable urate oxidase activity or protein in homozygous mutant (−/−) mice. (*A*) Homozygous mutant (−/−) mice lacked urate oxidase activity. Liver extracts from wild-type (●), heterozygous (○), and homozygous (△) mice were prepared and added to a reaction mixture containing uric acid. Urate oxidase activity was determined by measuring the rate of decrease in A_{292}, indicating the consumption of uric acid. Each point represents the average of simultaneous duplicate assays. (*B*) Urate oxidase protein in wild-type (+/+), heterozygous (+/−), and homozygous (−/−) mice. Urate oxidase protein was partially purified from mouse liver by homogenization and centrifugation. Arrowhead indicates the position of mouse urate oxidase protein, 33 kDa, in an SDS/12% polyacrylamide gel; this protein is missing in the homozygous mutants. Lane p, purified pig liver urate oxidase, 32 kDa, which is 1 kDa smaller than that of the mouse (21).

Development of Hyperuricemia and Urate Nephropathy in Mutant Mice. Urate oxidase-deficient mice developed pronounced hyperuricemia and marked hyperuricosuria (10 times more urinary uric acid than normal mice). Gross necropsies showed that lesions were confined to the kidneys. The kidneys from wild-type and heterozygous mice were normal in appearance, with a smooth cut surface. In contrast, progressive destruction of the kidneys from the homozygous mutants was observed during postnatal development. As early as 6 days after birth, small cortical cysts and white-yellow deposits could be seen in the hemisected kidneys. The deposits were usually manifested as linear streaks in the cortex but also occurred in the medulla. They stained weakly positive for uric acid by Gomori's silver method. However, when sections were stained with ethanolic eosin and then viewed microscopically under polarized light, the lesions were seen as crystalline, anisotropic structures consistent with uric acid crystals (Fig. 5). As the disease progressed, the affected kidneys became smaller, discolored (pale yellow), and soft. The surface of the kidney became irregular with obvious pits and scars. Multiple cysts were observed on the cut surface. Microscopically, tubular degeneration and regeneration with dilation of tubules were observed at 8 days of age. Urate crystals persisted until 14 days and then gradually resolved. As the obstructive disease progressed, hydronephrotic lesions appeared and resulted in severe hydronephrosis at 5 weeks. Cortical cysts started as dilations within the collecting tubules and extended from the papilla to the corticomedullary junction. These lesions persisted through adult life. Glomerular atrophy and dilation of Bowman's spaces within glomeruli were associated with foci of tubular

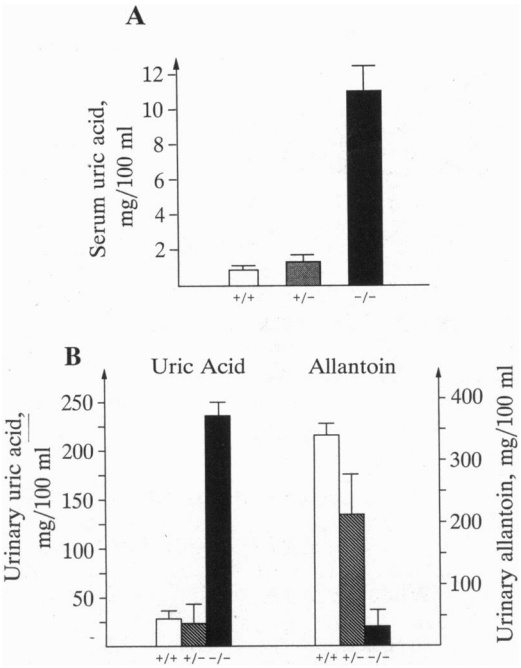

FIG. 4. Increased uric acid and decreased allantoin in urate oxidase-deficient mice. (*A*) Uric acid is increased in urate oxidase-deficient mice. Serum samples were collected from 3- to 4-week-old mice (5–10 mice in each group) and uric acid levels were measured spectrometrically by enzymatic reaction. The uric acid levels (mg/100 ml) were 11.0 ± 1.7 for the homozygous, 1.4 ± 0.5 for the heterozygous, and 0.9 ± 0.3 for the wild-type mice. (*B*) The increase in uric acid in the mutants coincides with a decrease in allantoin. Urine samples were collected from 5- to 6-week-old mice, and uric acid and allantoin were measured.

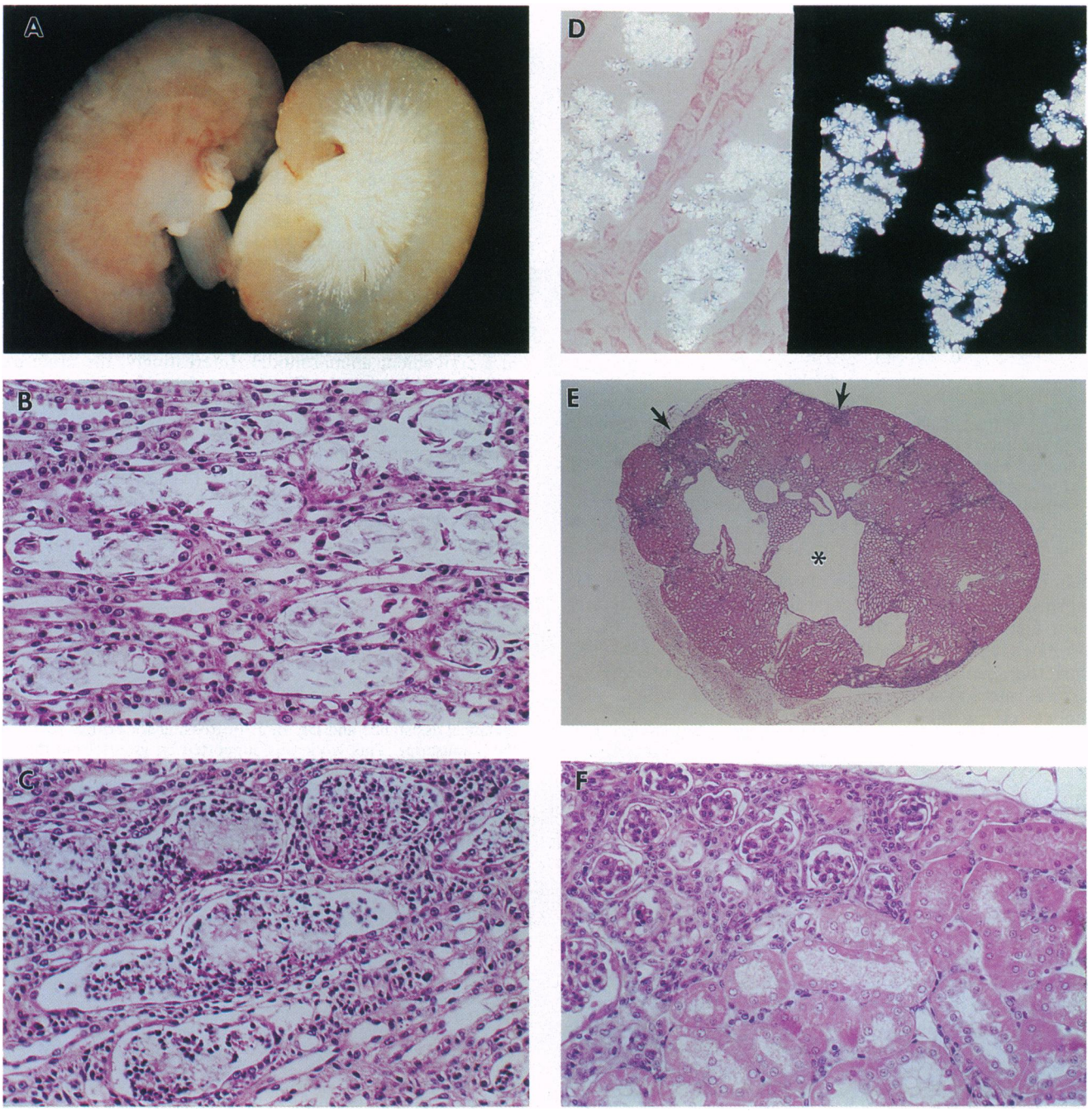

FIG. 5. Pathology of urate nephropathy in urate oxidase-deficient mice. (*A*) Gross photograph of normal wild-type kidney on left and kidney from a urate oxidase-deficient mouse on the right with linear white streaks in lower cortex and medulla representative of urate deposits in renal tubules and collecting ducts. (*B*) Microscopic view of dilated renal tubules containing bluish-pink material (urate crystals) and desquamated tubular epithelia in lumina. (Hematoxylin and eosin stain; ×40.) (*C*) Acute tubular necrosis with infiltration of neutrophils at day 14. (×20.) (*D*) Partial polarization of eosin-stained, ethanol-fixed kidney demonstrating anisotropic urate crystals in renal tubules on left and same field under full polarization on right. (×110.) (*E*) Subgross view of kidney at 5 weeks of age with moderate hydronephrosis (*) and blue foci in outer cortex (arrow). (×5.) (*F*) Higher power of *E* demonstrating tubular atrophy and collapse on left with crowding of glomeruli compared with normal renal tubules on right. (×40.)

atrophy and collapse of the nephron. Chronic inflammation, characterized by infiltration of plasma cells, lymphocytes, and macrophages, occurred within the interstitium of the kidney (Fig. 5). These findings are not unlike acute hyperuricemia nephropathy described in man.

Decreased Uric Acid Levels and Enhanced Survival Rate in Mutant Mice Treated with Allopurinol. Allopurinol, an inhibitor of xanthine oxidase, is widely used in the treatment of gout and hyperuricemia (23). The effect of allopurinol treatment on weaned mice was explored by administration of allopurinol in drinking water. Uric acid levels were measured before and after 2 weeks of treatment. Serum uric acid in treated homozygous mice decreased in a dose-dependent manner (Fig. 6). A 25% decrease in uric acid was observed with an allopurinol dose of 45 μg/ml. At 150 μg/ml, allopurinol decreased uric acid by about 50%.

Allopurinol was administrated to homozygous breeding pairs throughout the pregnancy and fostering period, and the survival rate of their offspring was analyzed at day 14. An enhanced survival rate was observed when the mice were

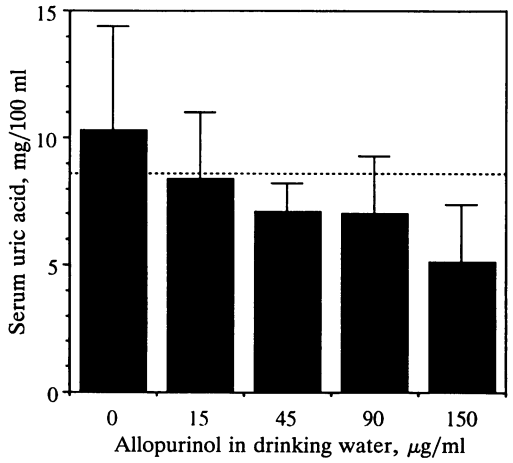

FIG. 6. Effect of allopurinol treatment on urate oxidase-deficient mice. The mice were weaned at 3 weeks of age and allopurinol was given for 2 weeks. Serum uric acid levels were measured before and after treatment. Data represent the mean ± SD of uric acid levels after treatment. Mean value of serum uric acid levels before treatment (8.6 ± 2.1 mg/100 ml, n = 48) is shown as a dotted line. Each group contained 6–11 mice.

treated with at least 45 μg of allopurinol per ml (Table 1). These studies suggest that allopurinol can protect newborns when administered to the mother, an observation which correlated with the transfer of allopurinol to breast milk. Thus, therapeutic benefit was observed in terms of newborn survival rate and serum uric acid in adult mice with allopurinol at ≥45 μg/ml in drinking water.

DISCUSSION

We have generated urate oxidase-deficient mice by homologous recombination in mouse ES cells. A null allele was created at the locus, judged by both protein and enzyme activity levels. The lack of urate oxidase in humans results in increased uric acid levels. As expected, uric acid levels in the urate oxidase-deficient mice were greatly increased (10-fold).

The destruction of the kidney was characteristic of mechanical blockage of renal tubules by urate crystal deposition within tubular lumens and subsequent obstructive nephropathy. Although urate nephropathy in mice is somewhat similar to gouty nephropathy in humans (23–25), there are certain differences. In mice, damage caused by urate crystals occurred much earlier in life and was more severe. As a result, a high lethality rate was observed in the urate oxidase-deficient mice during the first few weeks. The urate nephropathy associated with chemotherapy of hematopoietic malignancy is similar to these findings (26). We observed no tophi or joint urate depositions in the mice over the 1- to 4-week period.

Excessive quantities of uric acid in humans are associated with hyperuricemia and gout. The presence of urate oxidase in most other mammals prevents them from being used as animal models for the human disorders. The urate oxidase-deficient mice described here developed hyperuricemia and urate nephropathy that resemble some symptoms of gout in humans. Therefore, these mutant mice may be useful animal models for the human disease and should be useful in the development of therapy for hyperuricemia, including new drugs and uricase gene transfer, and in the study of uric acid metabolism and transport in mammals.

Purine metabolism is critical for the normal function of cells, and many defects in this pathway are related to human diseases such as Lesch–Nyhan syndrome, Down syndrome, and certain forms of mental retardation associated with autism. The urate oxidase-deficient mice contain a purine metabolic pathway similar to that of humans. Therefore, analysis of regulation of this pathway can now be undertaken in a convenient animal model. Interestingly, the urate oxidase-deficient mice also displayed a genetic variation in their purine metabolism as seen in humans.

Table 1. Allopurinol intervention study

Allopurinol in drinking water, μg/ml	No. of breeding pairs	No. of pups born alive	Death incidence, %		Survival at day 14, %
			Birth–day 7	Day 8–Day 14	
0	12	96	13.5	21.8	64.6
15	2	27	11.1	63.0	25.9
45	2	42	2.4	14.3	83.3
90	1	19	5.3	0	94.7
150	2	59	11.9	3.4	84.7

Given its absence, urate oxidase is presumably a nonessential enzyme in humans. Although lack of this enzyme can contribute to the development of hyperuricemia and gout in adult life, most humans do not develop the disease except in conjunction with other factors. In contrast, our results showed that the loss of urate oxidase alone in mice resulted in severe kidney damage and increased lethality at an early stage, indicating that urate oxidase plays a vital role in the clearance of uric acid in mice. Therefore, urate oxidase is an essential enzyme in the mouse and possibly in other mammals that retain the enzyme.

We thank Drs. C. C. Lee and H. Zheng for helpful suggestions and critical reading of the manuscript. We thank Dr. T. K. Moore for technical assistance and Dr. B. J. F. Rossiter for critical review of the manuscript. This work was supported by grants from the National Institute of Diabetes and Digestive and Kidney Diseases and the Howard Hughes Medical Institute. C.T.C. and A.B. are investigators with the Howard Hughes Medical Institute.

1. Florkin, M. & Duchatean, G. (1943) *Arch. Int. Physiol.* **53**, 267–306.
2. Christen, P., Peacock, W. C., Christen, A. E. & Wackker, W. E. C. (1970) *Eur. J. Biochem.* **12**, 3–5.
3. Friedman, T. B., Polanco, G. E., Appold, J. D. & Mayle, J. E. (1985) *Comp. Biochem. Physiol.* **81B**, 653–659.
4. Wu, X., Muzny D. M., Lee, C. C., & Caskey, C. T. (1992) *J. Mol. Evol.* **34**, 78–84.
5. Gutman, A. B. (1965) *Arthritis Rheum.* **8**, 614–626.
6. Smyth, C. J. (1975) *Arthritis Rheum.* **18**, Suppl. 6, 713–719.
7. Keilin, J. (1959) *Biol. Rev.* **34**, 265–296.
8. Orowan, E. (1955) *Nature (London)* **175**, 683–684.
9. Proctor, P. (1970) *Nature (London)* **228**, 868.
10. Ames, B. N., Cathcart, R., Schwiers, E. & Hochstein, P. (1981) *Proc. Natl. Acad. Sci. USA* **78**, 6858–6862.
11. Thomas, K. R. & Capecchi, M. R. (1987) *Cell* **51**, 503–512.
12. Mansour, S. L., Thomas, K. R. & Capecchi, M. R. (1988) *Nature (London)* **336**, 348–352.
13. McMahon, A. P. & Bradley, A. (1990) *Cell* **62**, 1073–1085.
14. Robertson, E. J. (1987) in *Teratocarcinomas and Embryonic Stem Cells: A Practical Approach*, ed. Robertson, E. J. (IRL, Oxford), pp. 71–112.
15. Bradley, A. (1987) in *Teratocarcinomas and Embryonic Stem Cells: A Practical Approach*, ed. Robertson, E. J. (IRL, Oxford), pp. 113–151.
16. Conly, T. G. & Priest, D. G. (1979) *Prep. Biochem.* **9**, 197–203.
17. Priest, D. G. & Pitts, O. M. (1972) *Anal. Biochem.* **50**, 195–205.
18. Liddle, L., Seegmiller, J. E. & Laster, L. (1959) *J. Lab. Clin. Med.* **54**, 903–913.
19. Young, E. G. & Conway, C. F. (1942) *J. Biol. Chem.* **142**, 839–853.
20. Gomori, G. (1946) *Am. J. Clin. Pathol.* **16**, 177.
21. Wu, X., Lee, C. C., Muzny, D. M. & Caskey, C. T. (1989) *Proc. Natl. Acad. Sci. USA* **86**, 9412–9416.
22. Mikkelsen, W. M., Dodge, H. J. & Valkenburg, H. (1965) *Am. J. Med.* **39**, 242–251.
23. Wyngaarden, J. B. & Kelly, W. N. (1976) *Gout and Hyperuricemia* (Grune & Stratton, New York).
24. Talbot, J. H. & Terplan, K. L. (1960) *Medicine* **39**, 405–468.
25. Heptinstall, R. H. (1966) *Pathology of the Kidney* (Little, Brown, Boston).
26. Kjellstrand, C. M., Campbell, D. C., II, von Hartitzsch, B. & Buselmeier, T. J. (1974) *Arch. Intern. Med.* **133**, 349–359.